nature COMMUNICATIONS

ARTICLE

Received 14 Nov 2014 | Accepted 25 Jun 2015 | Published 14 Aug 2015

DOI: 10.1038/ncomms8926

Myristoylation confers noncanonical AMPK functions in autophagy selectivity and mitochondrial surveillance

Jiyong Liang[1], Zhi-Xiang Xu[2,3], Zhiyong Ding[1], Yiling Lu[1], Qinghua Yu[1], Kaitlin D. Werle[2], Ge Zhou[4], Yun-Yong Park[1,†], Guang Peng[5], Michael J. Gambello[6,†] & Gordon B. Mills[1]

AMP-activated protein kinase (AMPK) plays a central role in cellular energy sensing and bioenergetics. However, the role of AMPK in surveillance of mitochondrial damage and induction of mitophagy remains unclear. We demonstrate herein that AMPK is required for efficient mitophagy. Mitochondrial damage induces a physical association of AMPK with ATG16-ATG5-12 and an AMPK-dependent recruitment of the VPS34 and ATG16 complexes with the mitochondria. Targeting AMPK to the mitochondria is both sufficient to induce mitophagy and to promote cell survival. Recruitment of AMPK to the mitochondria requires *N*-myristoylation of AMPKβ by the type-I *N*-myristoyltransferase 1 (NMT1). Our data support a spatiotemporal model wherein recruitment of AMPK in association with components of the VPS34 and ATG16 complex to damaged mitochondria regulates selective mitophagy to maintain cancer cell viability.

[1] Department of Systems Biology, The University of Texas MD Anderson Cancer Center, 1515 Holcombe Boulevard, Houston, Texas 77030, USA. [2] Department of Medicine, Division of Hematology and Oncology, Comprehensive Cancer Center, University of Alabama at Birmingham, Birmingham, Alabama 35294, USA. [3] Department of Pathology, Key Laboratory of Pathobiology, Ministry of Education, Norman Bethune College of Medicine, Jilin University, Changchun 130021, China. [4] Department of Head and Neck Surgery, The University of Texas MD Anderson Cancer Center, 1515 Holcombe Boulevard, Houston, Texas 77030, USA. [5] Department of Clinical Cancer Prevention, The University of Texas MD Anderson Cancer Center, 1515 Holcombe Boulevard, Houston, Texas 77030, USA. [6] Division of Medical Genetics, Department of Pediatrics, University of Texas Health Science Center at Houston, Houston, Texas 77030, USA. † Present addresses: Department of Medicine, ASAN Institute for Life Sciences, ASAN Medical Center, University of Ulsan College of Medicine, Seoul 138-736, Korea (Y.-Y.P.); Emory University School of Medicine, 615 Clifton Road, Atlanta, Georgia 30322, USA (M.J.G.). Correspondence and requests for materials should be addressed to J.L. (email: jyliang@mdanderson.org) or to G.B.M. (email: gmills@mdanderson.org).

Macroautophagy, commonly referred to as autophagy, is a degradation mechanism that mediates the sequestration and destruction of a variety of endogenous and exogenous cellular components as well as microbial pathogens contributing to the maintenance of cell bioenergetic homeostasis, cytoplasmic quality control and defence against disease[1–3]. In mammalian cells, autophagy can be triggered by extracellular signals and intracellular perturbations mediated through multiple interconnected pathways with the mTOR and AMPK cascades playing important roles in nutrient-depletion-induced autophagy[4–8].

While nutrient withdrawal triggers autophagy-mediated non-selective bulk degradation of cytoplasmic contents, autophagy can also selectively mediate removal of specific organelles[3,9]. Under starvation conditions, however, mitochondria can escape degradation by autophagy despite donating membrane structures for the biogenesis of non-selective autophagosomes[10]. Indeed, cell starvation induces mitochondrial elongation and tubulation through phosphorylation-dependent Drp1 downregulation, which protects mitochondria from autophagy-mediated degradation[11,12]. In contrast, autophagy can mediate selective mitochondrial removal, a process known as mitophagy, during lineage differentiation or in response to mitochondrial damage[13–16]. Studies with depolarized mitochondria provide important insights into autophagy-mediated selective degradation of damaged mitochondria. On depolarizing mitochondrial damage, the mitochondrial resident protein kinase PINK1 is activated and recruits the protein ubiquitin E3 ligase Parkin to damaged mitochondria, where Parkin catalyses ubiquitination of a variety of mitochondrial proteins[13,17,18]. Since ubiquitinated proteins can be recognized by p62/SQSTM1, which also interacts with LC3 via its C-terminal LIR motif, p62 could potentially bridge damaged mitochondria and autophagosomes[19–21]. However, p62 is not essential for mitophagy[22], suggesting that additional mechanisms may deliver damaged mitochondria to autophagosomes or, alternatively, the autophagy machinery can be recruited to damaged mitochondria to mediate mitochondrial removal.

Although Parkin overexpression in cultured cells can effectively eliminate the majority of mitochondria on depolarizing stress, endogenous Parkin levels are not sufficient to mediate mitophagy in many cell types including murine embryonic fibroblasts (MEFs)[23,24], which, similar to Parkin knockout cells, do not exhibit mitochondrial aberrations that are indicative of defects in mitochondrial surveillance[25–28]. Thus, the physiological role of Parkin-mediated mitophagy in mitochondrial homeostasis is not fully understood[14,29,30]. Indeed, mitophagy can occur in a PINK-Parkin cascade-independent manner[31–35], although the mechanisms of Parkin-independent mitochondrial surveillance remain to be elucidated.

Despite the striking difference in substrate selectivity between starvation and mitochondrial damage-induced autophagy, our data show that AMPK is activated under both conditions. AMPKα knockout cells exhibit suboptimal autophagy induction in response to multiple stress signals including depolarizing mitochondrial damage and exhibit defects in removal of damaged mitochondria. We demonstrate that the AMPK complex associates with damaged mitochondria, which is dependent on *N*-myristoylation of AMPKβ subunits. Further, mitochondrial damage induces physical interaction between AMPK and ATG16 complexes. AMPK is also required for retention of the ATG16 complex in damaged mitochondria. Thus, we provide evidence suggesting that association of AMPK with damaged mitochondria mediates recruitment of the ATG16 complex to the damage sites, serving as a new mechanism underpinning surveillance of mitochondrial damage and removal of damaged mitochondria through autophagy.

Results

AMPK plays a role in autophagy and mitochondrial removal. AMPK mediates adaptive cell functions in response to perturbations in nutrient metabolism and bioenergetics to maintain adequate intracellular energy levels[36]. AMPK plays an important role in regulating autophagy[5,37], a cellular process that provides energy during nutrient starvation. Given the variety of signals in addition to nutrient depletion that induce autophagy, we speculated that AMPK might be required for autophagy generally or alternatively only a subset of autophagy contexts. In MEFs, short-term serum or glucose starvation and brief treatment with either rapamycin or the mitochondrion-depolarizing agent CCCP (carbonyl cyanide 3-chlorophenylhydrazone) for 4 h increased LC3-PE (Fig. 1a), indicating that these conditions trigger a rapid onset of autophagy. Rapamycin but not glucose starvation or CCCP led to a marked reduction in pS6 levels (Supplementary Fig. 1A); thus, glucose starvation and CCCP-induced autophagy do not require substantial mTOR inhibition as represented by decreases in pS6 levels. Phosphorylation of AMPK (pAMPK) and AMPK substrates including ACC (pACC) and ULK1 (pULK)[38,39] was readily detected in wild-type, but not MEF cells lacking both AMPKα1 and α2 (AMPK −/−) (Fig. 1a; Supplementary Fig. 1A,L), indicating that these events are dependent on AMPK. In wild-type MEFs, CCCP induced pAMPK and pACC within 30 min (Supplementary Fig. 1B,C). LC3 lipidation was reduced (approximately two- to sixfold) and high-molecular-weight ubiquitinated proteins were substantially increased in AMPK −/− cells as compared with wild-type cells (Fig. 1a), suggesting altered autophagy activity[40–42]. LC3-PE levels remained lower in AMPK −/− cells in the presence of bafilomycin, which was used to clamp autophagosomes, suggesting that autophagy flux is not increased in these cells (Supplementary Fig. 1D).

AMPK promotes cell survival under nutrient starvation[5]. We observed rapid cell death in AMPK −/− but not wild-type MEFs treated with CCCP (Fig. 1b,c; Supplementary Fig. 1E), suggesting that AMPK also contributes to cell viability following mitochondrial damage. Similar results were obtained with RNA interference (RNAi)-mediated AMPKα depletion from H23 human lung cancer cells (Fig. 1d; Supplementary Fig. 1F,G). Further, CCCP-induced cell death was effectively prevented by reactive oxygen species scavenging and cell death-associated poly (ADP-ribose) polymerase1 (PARP1) cleavage was largely abolished by transfection of green fluorescent protein (GFP)-AMPKα2 in AMPK −/− cells (Fig. 1b,c). Taken together, AMPK is required for effective autophagy and cell survival in response to multiple signals including mitochondrial stress.

Transmission electron microscopy was performed to examine whether AMPK is required for autophagy-mediated removal of damaged mitochondria. As compared with wild-type MEFs, increased mitochondrion numbers and elongated mitochondria were present in AMPK −/− cells (Fig. 1e; Supplementary Fig. 1H). A brief exposure to CCCP led to mitochondrial swelling and altered or loss of cristae in the majority of mitochondria in both wild-type and AMPK −/− cells (Fig. 1e; Supplementary Fig. 1H–J). However, large-sized (>1 μM) mature autophagosomes containing mitochondrial vestiges (hereby termed mitophagosomes), often adjacent to clusters of curved or circular mitochondria, were present in wild-type but not AMPK −/− cells. Instead, relatively small non-selective autophagosomes devoid of recognizable organelles and autophagy-related structures (<0.5 μM) likely representing phagophores formed in AMPK −/− cells (Fig. 1e; Supplementary Fig. 1H–J).

To determine whether preautophagosomal vesicles formed in AMPK −/− cells might eventually develop into mature autophagosomes or the autophagy process might terminate

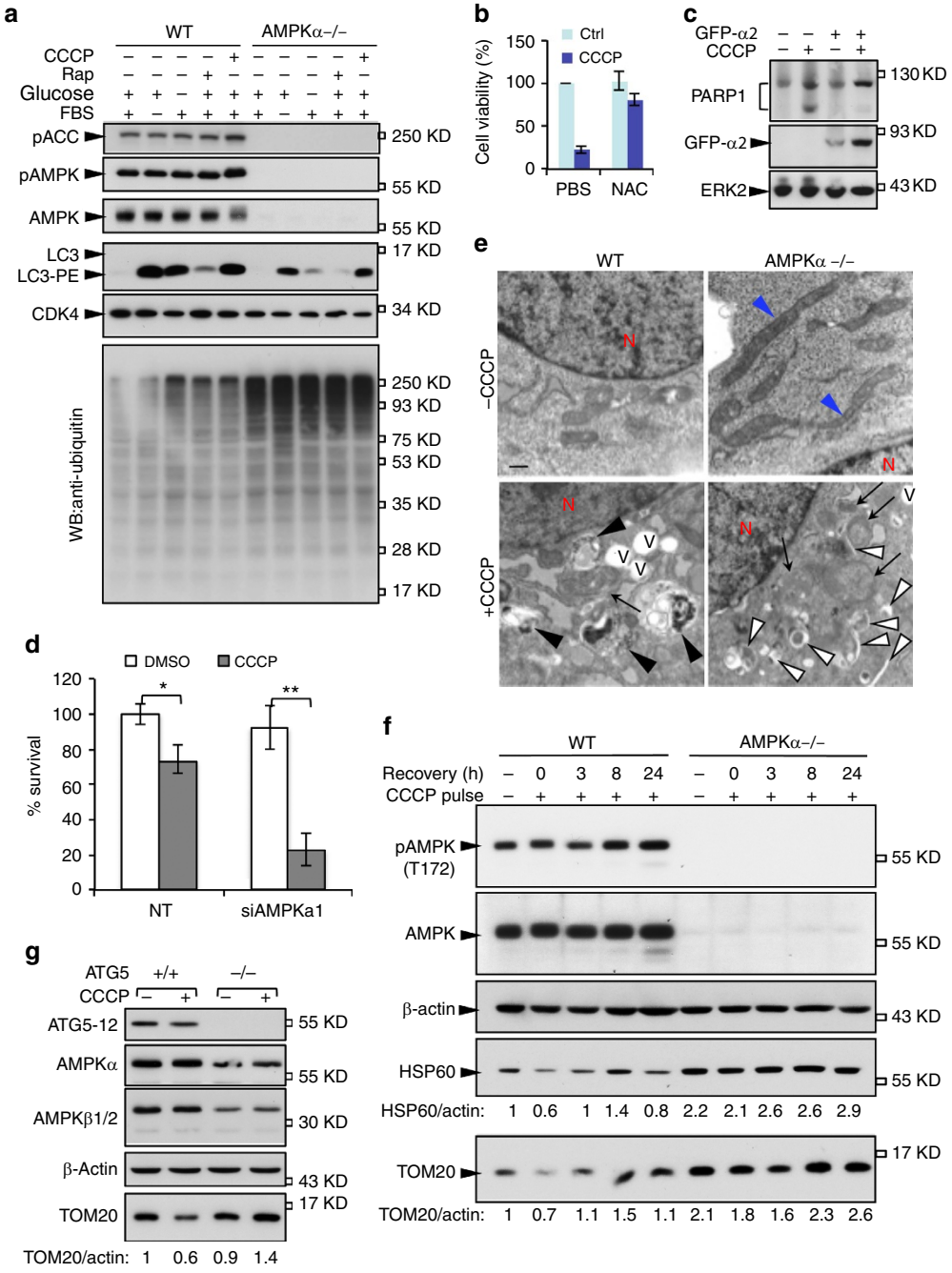

Figure 1 | AMPK-deficient cells exhibit suboptimal activation of selective and non-selective autophagy and rapid loss of cell viability on mitochondrial stress. (**a**) Western analyses of protein extracts from wild-type (WT) and AMPK −/− MEFs induced to undergo autophagy with various stimuli for 4 h. (**b**) Relative AMPK −/− cell viability determined by MTT assays treated with (+) or without (−) CCCP (5 μM, 72 h) in the presence or absence of *N*-acetyl-L-cysteine (NAC, 5 mM). (**c**) Western analysis of PARP1 cleavage in AMPK −/− cells transfected with (+) or without (−, mock) GFP-AMPKα2 (GFP-α2) following treatment with (+) or without (−) CCCP (30μM, 3 h). ERK2 was blotted for loading control. (**d**) Relative cell viability determined by CellTiter-Blue assays in NCI-H23 lung cancer cells transfected with non-targeting (NT) or AMPKα1 siRNAs for 48 h followed by treatment with CCCP (15μM) for additional 8 h. Control cells were incubated with vehicle (dimethylsulphoxide) only. Error bar, s.d. of four repeats; $^{*}P<0.05$; $^{**}P<0.01$ (Student's *t*-test). (**e**) Representative transmission electron microscopy microgrpahs of WT and AMPK −/− MEFs treated with or without CCCP (15 μM) for 4 h. Blue triangles, elongated aberrant mitochondria; arrows, damaged mitochondria; open triangles, isolation membranes and non-selective autophagosomes; black triangle, mature autophagosomes and mitophagosomes; N, nucleus; V, vacuoles; scale bar, 500 nM. High-magnification images are shown in Supplementary Fig. 1H. (**f**) Western analyses of protein levels from WT and AMPKα null (AMPKα −/−) MEFs briefly exposed to CCCP (30 μM for 2 h) and then allowed to recover for 3–24 h after the removal of CCCP at 0 h. (**g**) Western analyses of protein levels from WT and ATG5 −/− MEFs treated without (−) or with (+) CCCP for 3 h. Densitometry values of mitochondrial marker HSP60 and TOM20 by ImageJ (normalized against actin) were shown below each band.

prematurely after initiation, we performed a pulse-chase study. Following a transient exposure to CCCP, mitophagosomes and non-selective autophagic structures in wild-type and AMPK −/− cells, respectively, became less abundant following CCCP removal (Supplementary Fig. 1I–K). However, condensed mitochondrial fragments but not mitophagosomes were present in AMPK −/− cells, suggesting that cells lacking AMPK were unable to effectively remove damaged mitochondria through autophagy. Indeed, western analyses revealed reduced basal and CCCP-induced LC3-PE levels in AMPK −/− MEFs compared with wild-type cells. Following a transient CCCP pulse, LC3-PE returned to basal levels more rapidly (between 2 and 4 h) in AMPK −/− cells than in wild-type cells (~8 h) (Supplementary Fig. 1L). Thus, our data suggest that AMPK, while not obligatory for autophagy initiation, controls autophagy activity and signal duration. Consistent with inefficient elimination of damaged mitochondria, basal levels of the mitochondrial protein TOM20 were increased greater than twofold in AMPK −/− MEFs (Fig. 1f). Exposure to CCCP led to rapid loss of TOM20 and the mitochondrial chaperone HSP60 followed by a gradual recovery after CCCP removal in wild-type cells. In contrast, TOM20 and HSP60 levels underwent little change in AMPK −/− cells (Fig. 1f). Of note, loss of mitochondrial proteins preceded transient AMPK activation at the 4-h recovery time point (Supplementary Fig. 1L), likely due to a transient decline of ATP levels following extensive mitophagy and the restoration of ATP levels afterword due to either compensatory activation of glycolysis or *de novo* mitochondrial biogenesis. TOM20 levels were not reduced in ATG5 −/− cells on CCCP treatment (Fig. 1g), suggesting that loss of TOM20 is dependent on autophagy. Taken together, our data are consistent with a role for AMPK in autophagy-mediated mitochondrial removal.

LKB1 but not AMPK activity is dispensable for mitophagy. We next sought to determine whether LKB1, which plays a critical role in the energy-sensing cascade[43], is required for mitophagy. Following a brief exposure to CCCP, pACC was strongly induced in a panel of cell lines except for H23, which lacks functional LKB1 (Fig. 2a). Consistent with elevated pACC levels, LC3-PE was substantially increased following exposure to CCCP, whereas the 'autophagic flux' indicators p62 and NBR1 (in expressing cells) were decreased (Fig. 2a; Supplementary Fig. 2A). CCCP treatment did not alter p62 messenger RNA (mRNA) levels (Supplementary Fig. 2C).

The rapid autophagy induction in response to mitochondrial stress was accompanied by loss of mitochondrial proteins HSP60, COX-IV and TOM20 in H226 and H23 lung cancer cells (Fig. 2b; Supplementary Fig. 2A). However, COX-IV and HSP60 were not reduced in MDA-MB231 cells, whereas TOM20 levels were slightly increased in MCF7 cells (Fig. 2b; Supplementary Fig. 2A), despite comparable expression of Parkin, a protein ubiquitin E3 ligase that mediates ubiquitination-dependent mitophagy. Thus, MDA-MB231 and MCF7 cells undergo non-selective autophagy rather than mitophagy or, alternatively, mitochondrial biogenesis may compensate for the loss of specific mitochondrial proteins[22,44]. The substantial decreases in mitochondrial proteins following CCCP treatment in H23 cells lacking LKB1 is consistent with the LKB1-mediated energy-sensing function being dispensable for selective removal of damaged mitochondria. Phosphorylation of 4EBP1 remained unchanged in MDA-MD231 and H226 cells expressing functional LKB1 (Fig. 2a), suggesting that CCCP had little inhibitory effect on mTORC1. Unexpectedly, CCCP induced a substantial reduction in p4EBP1 in MCF7 and H23 cells (Fig. 2a), likely reflecting the loss of the 4EBP1 protein, the mechanism for which is currently unclear. These data argue that neither LKB1 nor mTORC1 inhibition is required for CCCP-induced mitophagy. Conversely, rapamycin-mediated mTOR inhibition resulted in loss of TOM20 in H226 but not H23 lung cancer cells (Supplementary Fig. 2B), consistent with mTOR inhibition alone being insufficient to initiate mitochondrial removal[33]. Further, short hairpin RNA (shRNA)-mediated depletion of LKB1 in SKOV3 cells had no effect on TOM20 downregulation, providing additional evidence supporting the notion that the energy-sensing function downstream of LKB1 is not required for mitophagy (Fig. 2c). In contrast, transfection of a kinase-dead mutant version of AMPKα, GFP-AMPKα2K45R, prevented CCCP-induced TOM20 downregulation in H23 cells (Fig. 2d), consistent with a requirement of AMPK kinase activity but not LKB1 in this process.

It is currently unclear why CCCP-induced AMPK activation was not sufficient to inhibit the mTORC1–4EBP1 cascade. Since CCCP treatment also caused striking increases in AKT phosphorylation (Supplementary Fig. 2B), mTORC1 activation might be maintained by a strong AKT activation following CCCP-induced mitochondrial stress, consistent with previous studies[45]. Indeed, allosteric inhibition of AKT with MK2206 suppressed S6 phosphorylation in CCCP-treated cells (Supplementary Fig. 2B).

Previous studies suggest a role for AMPK in regulating the ATG1 complex[46] and AMPK-dependent ULK1 phosphorylation regulates starvation-induced autophagy[38] and mitophagy in differentiated hepatocytes[39]. However, ULK1 phosphorylation is generally reduced during starvation-induced autophagy[7] with a sevenfold reduction in pULK1-S555 on nutrient starvation in cancer cells[47]. Although ULK1 phosphorylation at S555 (pULK1-S555), S777 (pULK1-S777) and S467 (pULK1-S467) was detected only in wild-type but not AMPK −/− cells (Supplementary Fig. 1A,L), pULK was not increased on CCCP treatment in any cell line tested and indeed pULK1-S555 was decreased following CCCP treatment in most cell lines (Fig. 2a; Supplementary Fig. 2B).

CCCP induces AMPK association with damaged mitochondria. To elucidate the mechanisms by which AMPK contributes to selective removal of damaged mitochondria, we determined whether AMPK might physically associate with mitochondria. We observed vesicle-like distribution of ectopically expressed GFP-AMPKα2 or RFP-AMPKα2 in the cytoplasm of approximately one-third of transfected cells. While these vesicular structures partially co-localized with the autophagosome marker, GFP-LC3 puncta, the vast majority of the vesicles overlapped with mCherry-p62 (Supplementary Fig. 3A,B), morphologically resembling both mitochondrial aggregates and autophagosome-related p62 bodies[19,21]. Similar subcellular distribution has been reported for AMPKβ subunits[48,49]. Indeed, transfection of AMPKβ1-GFP exhibited co-localization with MitoTracker Red (MTR) in Saos2 cells and the co-localization was increased by a short exposure to CCCP (Supplementary Fig. 3C).

To determine whether endogenous AMPK is recruited to the mitochondria in non-transfected cells, immunofluorescence staining was performed in MEFs. AMPKα subcellular distribution patterns overlapped with MTR in wild-type MEFs but not in AMPK −/− MEFs (Supplementary Fig. 3D,E). Further, mitochondrial extracts from several cell lineages were analysed for AMPK content. Total and T172-phosphorylated AMPK were readily detected in the mitochondrial fraction of all cell lines assessed including MEF and MCF7 cells (Fig. 3a,b). CCCP treatment led to an approximately threefold increase in AMPK in mitochondrial extracts (Fig. 3b), suggesting that AMPK is recruited to the mitochondria in response to mitochondrial damage. The mitochondrial protein porin (VDAC1) was

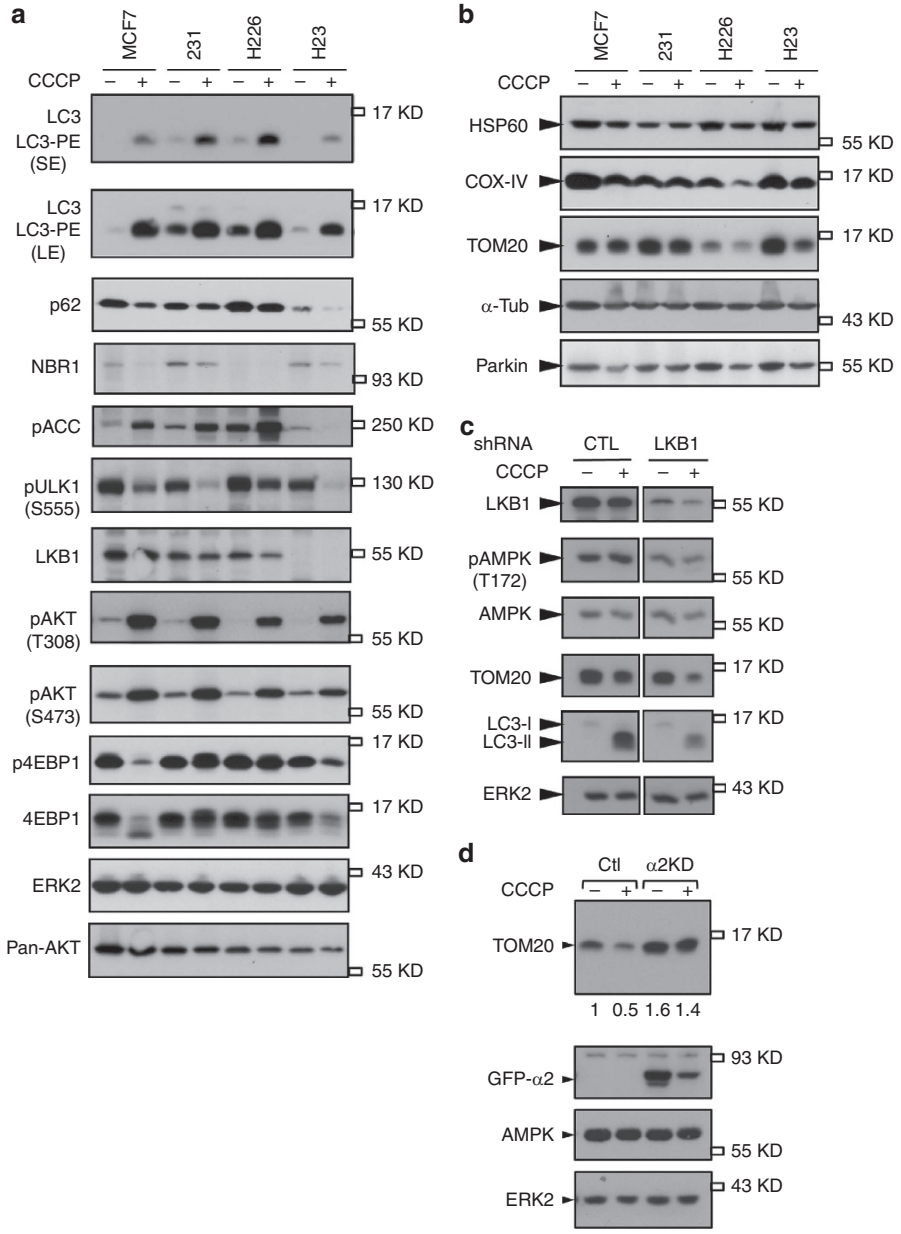

Figure 2 | LKB1 and mTORC1 inhibition are dispensable for mitochondrial autophagy in cancer cells. (**a**,**b**) Western analyses of cellular proteins extracted from human cancer cells treated with or without CCCP (30 μM) for 4 h. LE, longer exposure; SE, short exposure. (**c**,**d**) Western analysis of protein levels from SKOV3 (**c**) and H23 (**d**) cells transfected with either control (Ctl) or LKB1 targeting shRNA (**c**) or kinase-dead (K45R mutant) GFP-AMPKα2 (α2KD) (**d**) following treatment with (+) or without (−) CCCP for 4 h. Relative densitometry values (ratio to control, lane 1) as determined by ImageJ were shown below TOM20 blot (average of three independent experiments).

~10-fold enriched in the mitochondrial fraction and the cytosolic proteins, p70S6K, LKB1 and PDK1, were undetectable in the mitochondrial fraction (Fig. 3a,b), consistent with high purity of the mitochondrial preparation. To further validate the quality of mitochondrial isolation, reverse-phase protein array (RPPA) was performed to quantitatively determine the levels of multiple cellular and mitochondrial proteins. A number of mitochondrial proteins were enriched 2–12-fold in the mitochondrial extracts, whereas proteins not previously shown to be mitochondrial were detected at only background levels (Supplementary Fig. 3F,G). In addition, some proteins exhibited differential localization dynamics in a cell-type-dependent manner including the presence of pAKT in mitochondria in MCF7 (Fig. 3b), consistent with previous reports[50,51].

AMPK recruits mitophagy mediators. We next attempted to identify potential AMPK target(s) at the mitochondria that could mediate mitophagy. AMPK was previously shown to interact with the ULK1 complex[39,46]. However, dissociation of AMPK from the ULK1 complex is crucial for rapid autophagy induction on nutrient depletion in cancer cells[47]. We were unable to detect a steady-state interaction between endogenous ULK1 and AMPK in several cell types by co-immunoprecipitation; under the same condition, AMPKα was strongly associated with β subunits (Fig. 3c; Supplementary Fig. 3H). Given our data suggesting a role for AMPK in regulating the elongation steps leading to the formation of mature autophagosomes rather than preautophagosomal structures (Fig. 1e; Supplementary Fig. 1H–J), we then assessed potential physical interaction of AMPK with the

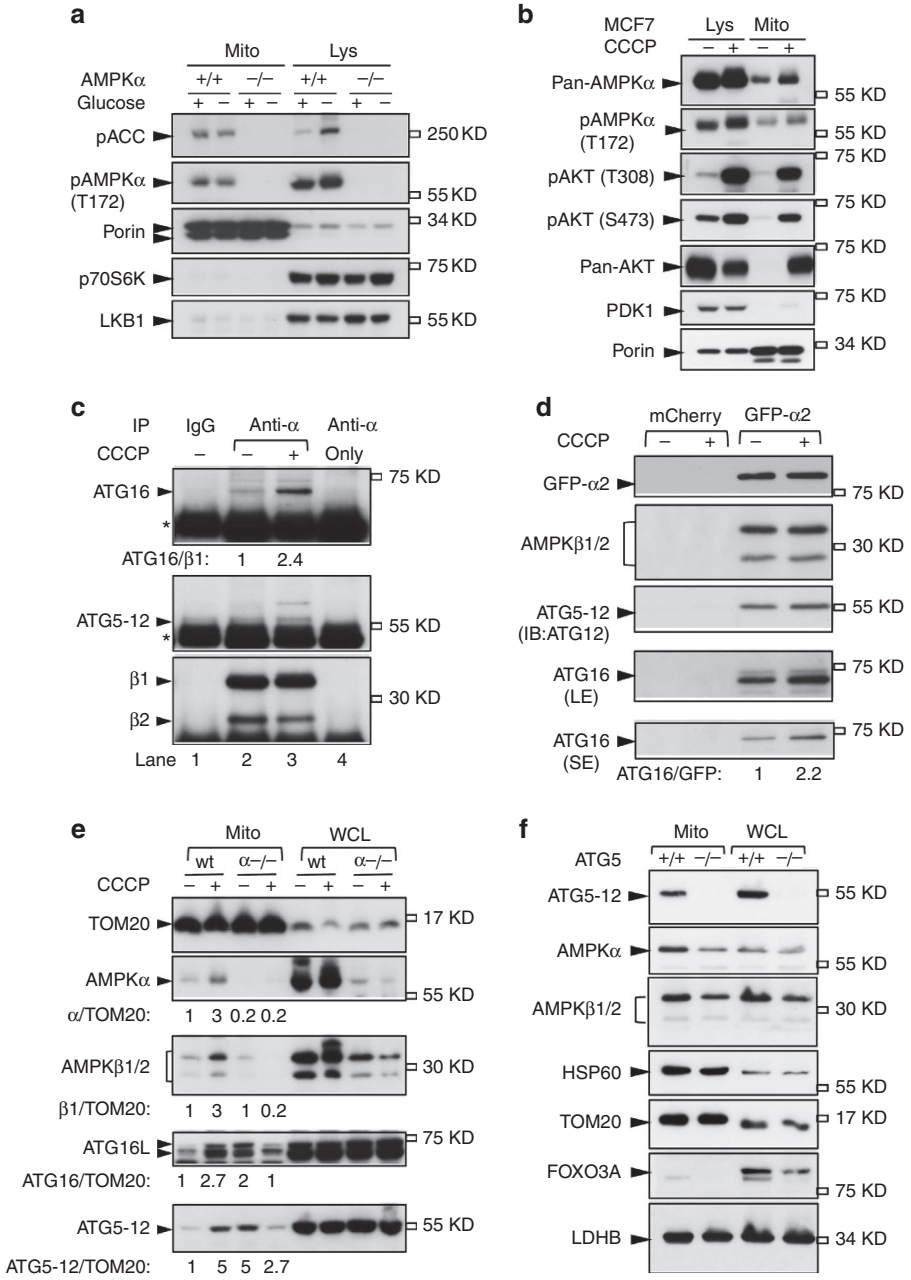

Figure 3 | Mitochondrial damage induces AMPK association with mitochondria and the ATG16 complex. (**a**,**b**) Western analyses of protein levels of whole-cell (Lys) and mitochondrial extracts (Mito) from wild-type (+/+) and AMPKα−/− MEFs cultured in the presence (+) or absence (−) of glucose (3 g l^{-1}) (**a**) and from MCF7 cells treated with (+) or without (−) CCCP (30 μM) (**b**) for 3 h. (**c**) Western analysis of proteins co-immunoprecipitated with AMPKα in MDA-MB231 cells. Control and mock precipitations were performed using either normal mouse IgG (IgG, lane 1) or the anti-AMPKα antibody only (no lysate, lane 4). * denotes heavy chain. The blots were probed sequentially in the order of ATG16, ATG12 and AMPKβ1/2. Note that only probing with ATG16 antibody (rabbit polyclonal) gives strong heavy chain signals, but not with ATG12 or the β1/2 antibodies (rabbit monoclonal) (Supplementary Fig. 3H). (**d**) Western analyses of proteins co-purified with GFP-AMPKα2 (GFP-α2) by GFP-TRAP assays from H23 stable lines following treatment with (+) or without (−) CCCP (30 μM, 4 h). Mock assays were performed as controls in cells transfected with an empty mCherry (mCh) vector. Note that GFP only control was shown in Supplementary Fig. 3I. LE, long exposure; SE, short exposure. (**e**,**f**) Western analyses of protein levels in whole cell lysate (WCL) or mitochondrial extracts (mito) from wild-type (wt) or AMPKα−/− (α−/−) MEFs treated with or without CCCP (15 μM) for 3 h (**e**) and from wild-type and ATG5−/− MEFs (**f**). Cytosol and nuclear protein FOXO3A and mitochondrial proteins HSP60 and TOM20 were blotted as fractionation controls.

VPS34 and ATG16 complexes. While there was no detectable interaction between VPS34 and AMPK, both ATG16 and ATG5-12 conjugates were present in AMPKα immunoprecipitates of endogenous proteins (Fig. 3c; Supplementary Fig. 3H). Notably, a brief CCCP treatment led to a two to over threefold increase in the ability to co-precipitate AMPK and ATG16 complexes (Fig. 3c; Supplementary Fig. 3H). The GFP-AMPKα2 fusion but not GFP alone also associated with the ATG16 complex (Supplementary Fig. 3I) with the interaction increasing greater than twofold on CCCP treatment (Fig. 3d). Further, to

determine whether AMPK kinase activity is required for association with the ATG5 complex, we performed stable transfection of wild-type and kinase-dead GFP-AMPKα2. Although wild-type and kinase-dead proteins are expressed at different levels with the latter being approximately twofold higher (Supplementary Fig. 3J), they form a complex with proportional amounts of β subunits (Supplementary Fig. 3K). Both fusion proteins are capable of association with ATG5-12, which is increased in response to CCCP. However, although AMPKα2KD was present in a complex with ATG5-12, relatively more ATG5-12 (approximately twofold) associates with wild-type AMPKα2 (Supplementary Fig. 3K), suggesting that AMPK activity accelerates the recruitment of the ATG5 complex following CCCP-induced mitochondrial damage.

We next interrogated whether AMPK regulates recruitment of the autophagy machinery. The core components of the class III PI3K complex VPS34-VPS15 and the ATG16-ATG5-12 complex, which mediate multiple steps of autophagy, were markedly increased in the mitochondrial fraction on CCCP treatment in wild-type cells (Fig. 3e; Supplementary Fig. 3L). These proteins were more abundantly detected in mitochondrial extracts from non-treated AMPK −/− cells compared with wild-type cells, likely due to the accumulation of damaged mitochondria and ubiquitinated proteins in these cells (Fig. 1a,e). However, in contrast to wild-type cells, CCCP treatment led to a slight decrease in the VPS34 complex and a loss of ATG16 complex from the mitochondria in AMPK −/− cells (Fig. 3e; Supplementary Fig. 3L). Further, while recruitment of core autophagy regulators to mitochondria requires AMPK, both AMPKα and β were present in mitochondria in ATG5 −/− MEF cells (Fig. 3f), suggesting that AMPK association with mitochondria is not dependent on association with ATG5 or autophagy, which is dependent on ATG5. Thus, our data are consistent with AMPK being required for retaining VPS34 and ATG16 complexes in damaged mitochondria on depolarizing stress.

Mitochondrial association requires *N*-myristoylation of AMPKβ. *N*-myristoylation of AMPKβ subunits is essential for AMPK association with intracellular membranes[49]; we posited that recruitment of the AMPK complex to mitochondria might be mediated through the same mechanism. In the majority (∼72%) of transfected MEF and H23 cells, AMPKβ1-GFP associated with vesicle structures, whereas the *N*-myristoylation-defective β1 mutant, AMPKβ1G2A-GFP, exhibited either homogenous distribution or distinct perinuclear aggregates varying in size partially co-localized with mCherry-p62 (Supplementary Fig. 4A). AMPKβ1-GFP but not AMPKβ1G2A-GFP co-localized with MTR, which was enhanced on CCCP treatment during autophagosome clamping with bafilomycin A1 (Supplementary Fig. 4B,C).

Consistent with the recruitment of AMPKβ1 but not AMPKβ1G2A to the mitochondria, we detected robust AMPKβ1 myristoylation in H23 cells in the mitochondrial fraction following labelling with amidomyristate using click chemistry (Fig. 4a). A brief exposure to CCCP led to a 1.6-fold increase in myristoylated AMPKβ1 in the mitochondrial fraction with a modest increase in overall levels of mitochondrial myristoylated proteins (Fig. 4b). We then examined whether protein myristoylation is required for damage-induced mitochondrial removal using the myristate analogue, 2-hydroxymyristic acid (2HMA). 2HMA inhibited mitochondrial protein myristoylation more effectively than cytosolic proteins as determined by click chemistry, with stronger inhibitory effects being achieved in the cells treated with CCCP (Fig. 4c). Strikingly, inhibition of myristoylation effectively abrogated membrane recruitment of the AMPK complex and the loss of COX-IV and TOM20 in response to mitochondrial damage (Fig. 4d). Note that although the Miro-1 GTPase, previously shown to be a target of Parkin-mediated proteolysis[52], also requires myristoylation for membrane association, its levels were not affected by CCCP arguing against a role of Parkin-dependent proteolysis in this setting (Fig. 4d; Supplementary Fig. 4D).

While myristoylation could potentially affect multiple mitochondrial proteins, the myristoylation-deficient form of AMPKβ1 (AMPKβ1G2A) was not present in mitochondria even in the absence of myristoylation inhibitor (Supplementary Fig. 4E), suggesting that the association of AMPK with mitochondria is intrinsic to *N*-myristoylation of the β subunits rather than being mediated through the myristoylation of other proteins. Strikingly, autophagosome clamping with bafilomycin revealed multiple mitophagosomes following a brief exposure to CCCP in H23 cells but not in cells pre-treated with 2HMA with 2HMA-treated cells containing a larger number of damaged mitochondria (Fig. 4e; Supplementary Fig. 4F). These data suggest a crucial role for protein *N*-myristoylation in mitophagy.

Association of AMPK with mitochondria mediates mitophagy. Since AMPKβ *N*-myristoylation does not affect AMPK complex formation[49], we postulated that the myristoylation-incompetent AMPKβ1G2A-GFP, due to its inability to associate with membranes and specifically mitochondria, might function in a dominant-negative manner if membrane association is required for AMPK to mediate mitophagy. We thus examined the effects of AMPK mislocalization on autophagy selectivity. AMPKβ1-GFP showed partial co-localization with mCherry-LC3 puncta in ∼31% of co-transfected cells; co-localization was enhanced over twofold on autophagosome clamping with bafilomycin A1 (Fig. 5a). AMPKβ1G2A-GFP did not co-localize with LC3 puncta in either the presence or absence of bafilomycin A1 (Fig. 5a). Further, CCCP-induced TOM20 loss was abolished in H23 cells transfected with AMPKβ1G2A-GFP but not the wild-type β1 subunit, whereas AMPKβ1G2A-GFP did not affect p62 turnover, LC3 lipidation or rapamycin-induced non-selective autophagy (Fig. 5b; Supplementary Fig. 5A). Thus, while myristoylation-mediated membrane association of the AMPK complex contributes to mitochondrial degradation, this mechanism is dispensable for non-selective autophagy.

We next determined whether forced mitochondrial localization of AMPK is sufficient to trigger mitochondrial removal. To constitutively target AMPK to mitochondria, we tagged AMPKβ1-GFP N terminally with the mitochondrial localization signal of TOM20 with the resultant construct being designated Mito-β1-GFP (Fig. 5c). Mito-β1-GFP exhibited co-localization with MTR (Fig. 5d), suggesting that Mito-β1-GFP is exclusively mitochondrial in the absence of mitochondrial stress. Strikingly, mitochondrial alterations were observed in all cells transfected with Mito-β1-GFP as compared with 39% of non-transfected cells (Fig. 5d) or 36% of the cells transfected with TOM20-GFP (Supplementary Fig. 5B,C), including loss of the peripheral portion of the mitochondria and disruption of mitochondrial network. To determine whether these aberrations might be due to mitophagy, we compared the effects of Mito-β1-GFP on mitochondria in wild-type versus ATG5 −/− MEFs. Similar phenotypes including loss of the bulk of the mitochondrial network were observed in wild-type MEFs but not ATG5 −/− cells (Fig. 5e; Supplementary Fig. 5D), suggesting that the mitochondrial alterations caused by mitochondrial-targeted AMPK are dependent on ATG5, which is essential for autophagy and mitophagy. The mitochondrial changes induced by Mito-β1-GFP were recapitulated when TOM20-mCherry was used to mark mitochondria (Supplementary Fig. 5E). Thus, our data

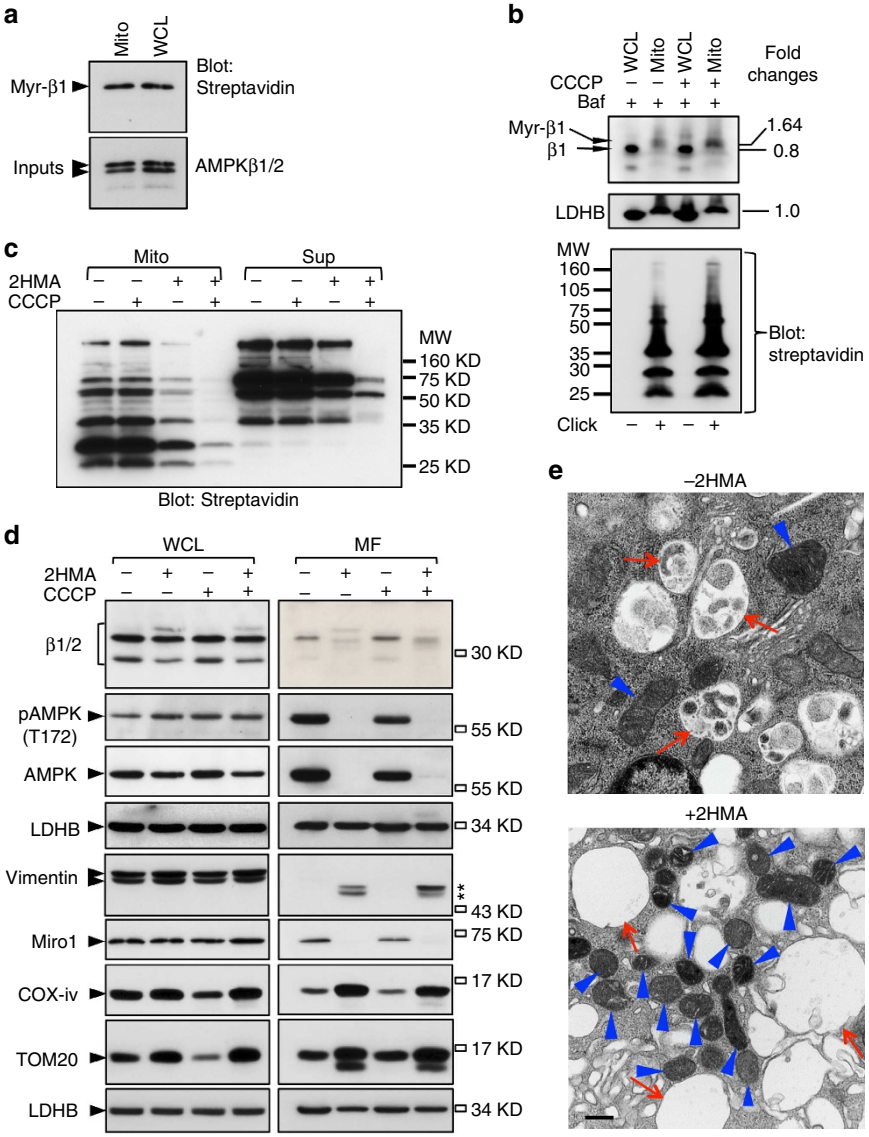

Figure 4 | Protein *N*-myristoylation is required for AMPK association with mitochondria and mitochondrial removal. (**a**) Detection of myristoylated AMPKβ1 (Myr-β1) co-precipitated with GFP-AMPKα2 following metabolic labelling of H23 cells with azidomyristate and *in vitro* conjugation with biotin alkyne. Input protein levels were determined by immunoblotting. Note that biotin-conjugated azidomyristoylated AMPKβ1 migrated relatively slowly. (**b**) Western analyses of myristoylated AMPKβ1 (Myr-β1) levels in the whole-cell lysate (WCL) and mitochondrial fraction (Mito) of H23 cells treated with or without CCCP following azidomyristic acid labelling and click chemistry. WCL without click conjugation was loaded as controls. Bafilomycin (Baf) was used to prevent autophagy/mitophagy-mediated protein degradation. LDHB was blotted for loading control. The bottom panel shows overall levels of protein myristoylation (streptavidin blot) in the mitochondria. ImageJ quantification was performed to assess the relative abundance of the proteins (fold changes). (**c**) Detection of overall levels of protein myristoylation in mitochondria (Mito) and cytosol (sup) following metabolic labelling and click chemistry in H23 cells treated with (+) or without (−) 2-hydroxy myristic acid (2HMA) and CCCP. (**d**) Western analyses of protein levels from H23 cells treated without (−) or with (+) CCCP (30 μM) for 4 h in the presence (+) or absence (−) of 2HMA (0.5 mM; added 20 h before CCCP). WCL, whole-cell lysate; MF, membrane fraction extracted using the Cell Fractionation Kit, HT (Ab109718) from Abcam (Cambridge, MA, USA). Note that AMPK complex was not enriched in the membrane fraction containing the plasma membrane and other organelles in addition to the mitochondria. ** denotes absence of vimentin in membrane fraction and presence of a faster migration band of non-characterized origin in 2HMA-treated cells. (**e**) Representative transmission electron microscopy micrographs of H23 cells treated with (+) or without (−) 2HMA (0.5 mM) for 24 h before brief exposure to CCCP (15 μM) in the presence of bafilomycin A (100 nM). Red arrows, autophagosomes; blue triangles, mitochondria; scale bar, 500 nM.

suggest that direct targeting of AMPK to mitochondria is sufficient to mediate autophagy-dependent mitochondrial removal.

The PINK-Parkin pathway mediates mitophagy with Parkin being recruited to mitochondria. We next determined whether AMPK-mediated mitochondrial removal requires Parkin. HCC38 human breast cancer cells, bearing a homozygous deletion of the *PARK2* gene[53], lack detectable expression of Parkin (Supplementary Fig. 5F). In HCC38 cells, CCCP induced loss of mitochondrial proteins TOM20 and CHCHD3 to an extent comparable to that observed in H23 cells (Supplementary Fig. 5F–H). Transfection of Mito-β1-GFP led to loss of the peripheral portion of the mitochondrial network (Supplementary Fig. 5I), similar to the phenotype found in Parkin expressing cells

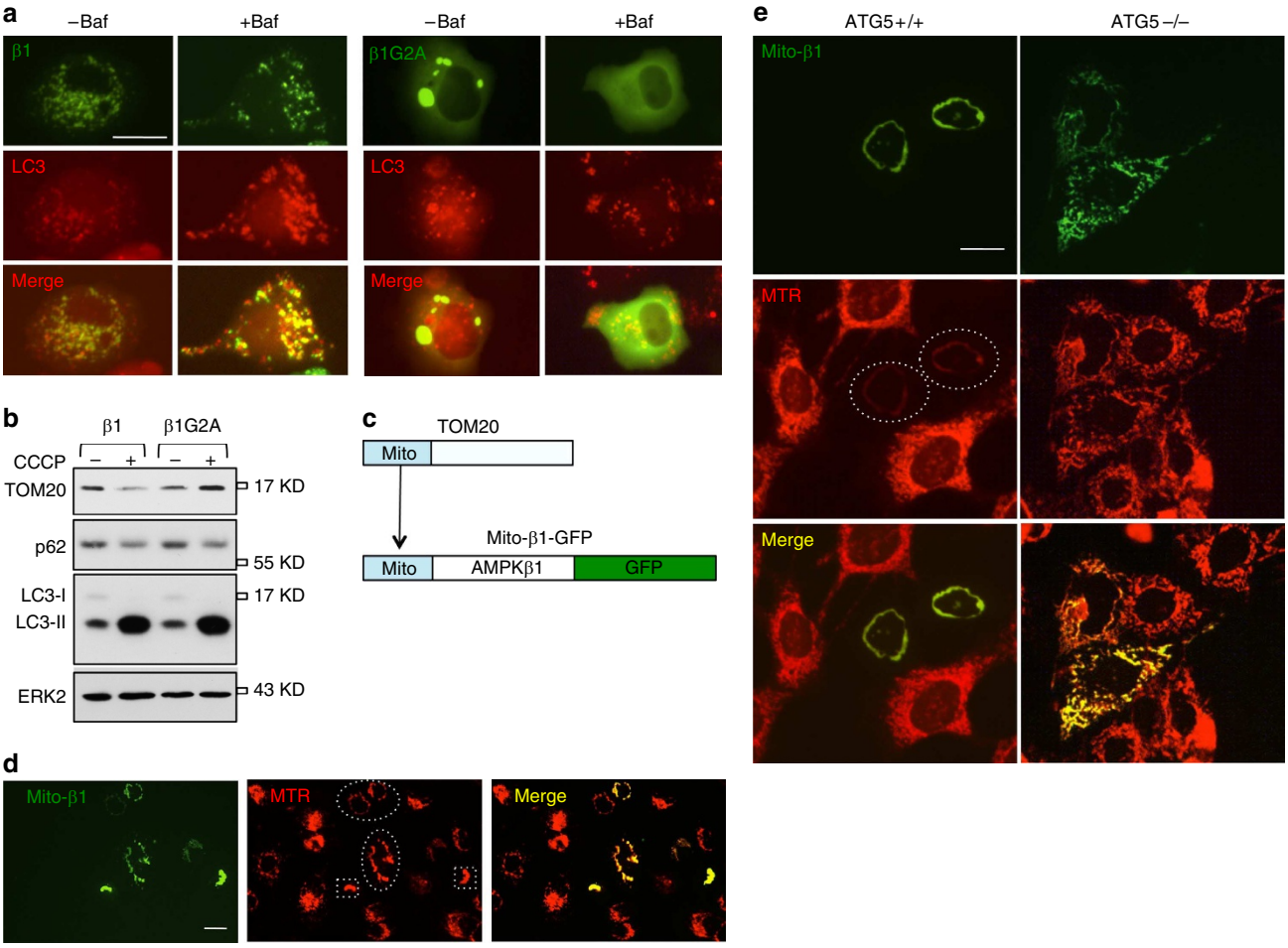

Figure 5 | AMPKβ1 myristoylation and mitochondrial AMPK mediate mitochondrial removal. (**a**) Subcellular localization of GFP-AMPKβ1 (β1) and the myristoylation defective mutant AMPKβ1G2A (β1G2A) and co-localization with mCherry-LC3 in the presence and absence of bafilomycin A1 (100 nM; 2 h). Scale bar, 20 μm. (**b**) Western analysis of TOM20 levels in H23 cells transfected with GFP-AMPKβ1 or GFP-AMPKβ1G2A treated with CCCP for 4 h. ERK2 was blotted for loading control. (**c**) The generation of mitochondrion targeting AMPKβ1 (Mito-β1-GFP) by N terminally tagging AMPKβ1-GFP with the mitochondrial localization signal (Mito) from TOM20. (**d**,**e**) H23 cells (**d**) and MEFs (**e**) transfected with Mito-β1-GFP with mitochondria stained with MitoTracker Red (MTR). Circled cells show typical mitochondrial alterations (loss of peripheral portion of the mitochondria and disruption of the mitochondrial network) that are not found in ATG5 −/− cells. Scale bar, 20 μm.

(Fig. 5d,e; Supplementary Fig. 5E). Further, knockdown of AMPKα impaired CCCP-induced loss of mitochondrial proteins in HCC38 cells (Supplementary Fig. 5J,K), consistent with a role of AMPK in mediating Parkin-independent mitophagy.

Mitophagy represents a surveillance mechanism against damaged mitochondria, which release reactive oxygen species and protein factors including cytochrome *c* that trigger the intrinsic apoptosis pathway. We posit that the inability to remove damaged mitochondria in a timely manner would cause apoptosis and potentiate the effects of apoptosis inducers. Indeed, incubation of H23 cells with 2HMA to prevent myristoylation of AMPK and subsequent recruitment to the mitochondria, inhibited cell growth effectively with prolonged exposure for 2 weeks eliminating the entire cell population (Fig. 6a), whereas myristic acid exhibited no cytotoxicity (Fig. 6b). Forced mitochondrial localization of AMPK using Mito-β1-GFP markedly improved cell viability (Fig. 6c), suggesting a role for mitochondrial AMPK in protecting cells from 2HMA-induced cell death. Further, 2HMA treatment for 48 h led to PARP1 cleavage and substantial loss of AMPK proteins (Fig. 6d; Supplementary Fig. 6A). While 2HMA alone induced a modest level of apoptosis-associated PARP1 cleavage and etoposide alone induced PARP1 cleavage only when used at a high dose (5 μM), the combination of 2HMA with a sub-lethal dose of etoposide (2.5 μM) caused a marked increase in PARP1 cleavage in H23 cells, leading to substantial loss of intact PARP1 (Fig. 6d; Supplementary Fig. 6A). These data suggest that protein *N*-myristoylation of AMPK promotes cell viability. To identify the enzyme(s) responsible for AMPK *N*-myristoylation, RNAi was performed to knockdown myristoyl-CoA protein *N*-myristoyltransferase 1 (NMT1) and NMT2. Depletion of NMT1 but not NMT2 led to AMPK loss (Fig. 6e), recapitulating the effects of 2HMA. Thus, it is likely that NMT1, but not NMT2, mediates AMPKβ *N*-myristoylation. Further, knockdown of NMT1 in H23 cells, while having little effect on autophagic flux as indicated by a comparable extent of CCCP-induced loss of p62 and induction of LC3-II, partially prevented the loss of TOM20 (Supplementary Fig. 6B). These data suggest a role of NMT1-mediated myristoylation in selective removal of mitochondria. Interestingly, NMT1 but not NMT2 is overexpressed in ~1/3 of human lung adenocarcinomas and high NMT1 mRNA levels correlate with statistically significantly poorer overall patient survival (Fig. 6f). The association of higher NMT1 mRNA levels

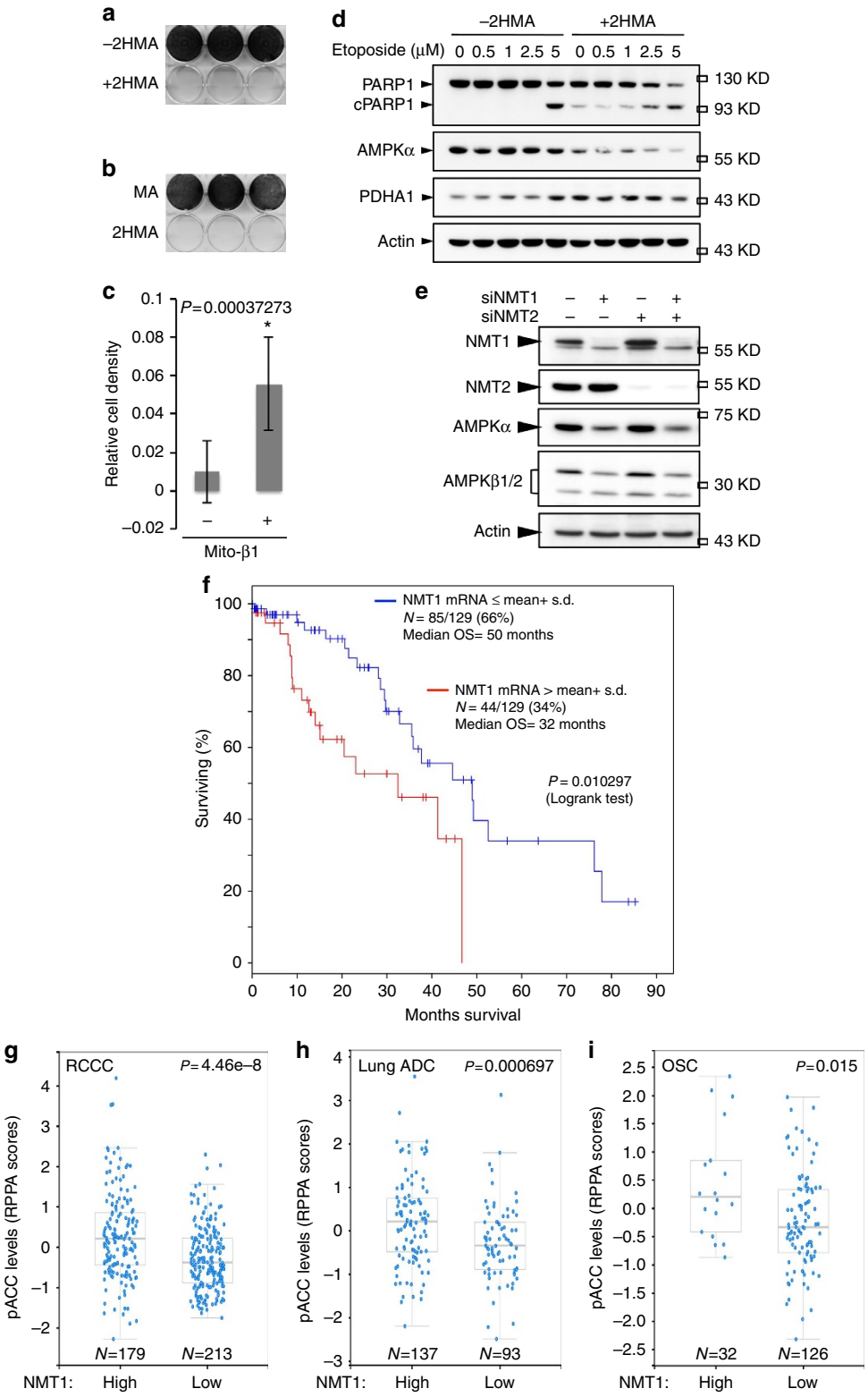

Figure 6 | Protein *N*-myristoylation plays a role in cancer cell survival and patient outcome. (**a**,**b**) H23 cells cultured in the presence or absence of 2-hydroxymyristic acid (2HMA 0.5 mM) or myristic acid (MA 0.5 mM) for 2 weeks. (**c**) Relative density of H23 cells transfected with either GFP only (−) or Mito-β1-GFP (+) treated with 2HMA (0.5 mM) for 2 weeks. *P* value was determined by Student's *t*-test. (**d**) Western analyses of protein levels in H23 cells treated without (0) or with increasing amounts of etoposide for 24 h in either the presence of or the absence of 2HMA added 24 h before etoposide. (**e**) Western analyses of protein levels in H23 cells transfected with non-targeting siRNA (−) and siRNAs targeting NMT1 and NMT2, respectively. (**f**) Kaplan–Meier estimates of overall patient survival (OS) of lung adenocarcinoma ((TCGA, provisional)/all complete tumours ($N=129$)). (**g**–**i**) pACC (S79) levels determined by RPPA assays in renal clear cell carcinoma (RCCC), lung adenocarcinoma (ADC) and ovarian serous cystadenocarcinma (OSC) tumours with high (>mean) and low (≤mean) NMT1 mRNA expression (TCPA data sets). Box represents the first to third quartile and whiskers represent 1.5 interquartile range. *P* values were calculated using Student's *t*-test.

with poorer patient outcomes was also found in ovarian (Supplementary Fig. 6C) and kidney cancers with progressively worsened patient survival linked to increasing NMT1 levels in renal clear cell carcinoma (Supplementary Fig. 6D). In all three tumour types where NMT1 levels predict poorer prognosis, high NMT1 mRNA expression strongly correlates with increased ACC phosphorylation (Fig. 6g–i), consistent with the AMPK-ACC cascade being downstream of NMT1, as AMPKβ myristoylation also regulates stress-induced AMPK activation in LKB1 proficient cells[49]. Indeed, the correlation between NMT1 mRNA and pACC levels was maintained in lung cancer samples with wild-type LKB1 ($P = 0.0038$) and LKB1 is rarely aberrant in either ovarian or renal cell cancer. Furthermore NMT1 knockdown in cancer cells expressing functional LKB1 led to a reduction in stress-induced ACC phosphorylation (Supplementary Fig. 6E). Thus, although LKB1 status and function remain to be determined in respective cancer tissues, there appears to be a broad relationship between NMT1 and pACC.

Discussion

The energy-sensing function of the LKB1-AMPK cascade can mediate starvation-induced autophagy, which lacks substrate selectivity[54], as well as mitochondrial biogenesis under energy stress[55–57]. We now provide several lines of evidence that AMPK plays a significant role in surveillance of mitochondrial stress by mediating selective removal of damaged mitochondria through autophagy. Our data, however, suggest that the role of AMPK in mitochondrial surveillance is independent of LKB1 and hence its energy-sensing function. Such functional specification can in principle mitigate signalling ambiguity by allowing selective removal of damaged mitochondria in the absence of energy stress and, conversely, preventing inadvertent mitochondrial depletion under nutrient starvation when mitochondrial function becomes critical for efficient bioenergetics.

In conjunction with the findings that AMPK regulates both selective and non-selective autophagy[39,46], we propose the existence of multiple mechanisms whereby AMPK regulates autophagy selectivity. In rapidly proliferating cells, AMPK appears to be required for the vesicle elongation step to form mature autophagosomes but not the initial step of autophagy that generates phagophores. Pre-autophagosome vesicles were present in greater numbers in AMPK−/− than in wild-type cells (Fig. 1e), suggesting that AMPK may function to achieve autophagy selectivity, in part, by limiting the formation of non-selective phagophores. In addition, we showed that AMPK along with the class III PI3K VPS34 and the ATG16-ATG5-12 complexes, which mediate vesicle elongation and autophagosome maturation, were actively recruited to mitochondria on depolarizing damage. Notably, mitochondrial stress triggers a rapid association between AMPK and the ATG16 complex, which appears to mediate the retention of the ATG16 complex and potentially additional proteins at damaged mitochondria. Both of the VPS34 and ATG16 complexes have multiple phosphorylated components with VPS34 and BECN1 being direct substrates of AMPK[58]; future studies are warranted to determine whether AMPK-dependent phosphorylation of these and additional targets plays a role in mediating mitophagy. Nonetheless, dynamic recruitment of AMPK, the VPS34 and ATG16 complexes to the mitochondria appears to facilitate the recruitment and lipidation of LC3, which is a substrate of the ATG16 complex[59]. In addition to being essential for LC3 lipidation, homotypic fusion of ATG16L1 precursors represents a critical step in autophagosome biogenesis before LC3 lipidation[59]. This notion is supported by the observation that targeting AMPK specifically to mitochondria was sufficient to induce loss of mitochondria in a manner that is dependent on ATG5, an essential component of the ATG16 complex (Fig. 5e). Thus, recruitment of AMPK to mitochondria may act to sense mitochondrial damage allowing assembly and activation of the autophagy machinery in temporal and spatial proximity to damage sites. This mechanism, although reminiscent of the translocation of Parkin to damaged mitochondria, differs from the role of the PINK-Parkin cascade, which appears to target damaged mitochondria to pre-formed autophagosomes through ubiquitination of mitochondrial proteins[14]. In addition, overexpression of Parkin can completely eliminate mitochondria in cells, which was not the case for AMPK. Indeed, our data suggest that AMPK can mediate mitophagy independent of Parkin, consistent with AMPK-mediated recruitment of the autophagy machinery to damaged mitochondria, representing a novel mitophagy pathway.

Of note, we found spatial association of AMPK with mitochondria and autophagosomes to be reliant on *N*-myristoylation of AMPKβ, which mediates membrane association[49]. In contrast, non-selective autophagy was not dependent on AMPK *N*-myristoylation compatible with the different roles for AMPK in selective and non-selective autophagy, being at least in part dependent on localization to specific organelles. Interestingly, *N*-myristoylation of Sip1, the yeast version of the AMPKβ subunit, is essential for the Snf1 complex to localize to vacuolar membranes on glucose withdrawal in *Saccharomyces cereviciae*[60]. Thus, this mechanism appears to be evolutionarily conserved. It is currently unclear how *N*-myristoylation mediates AMPK association with damaged mitochondria. Since protein lipidation is one of the mechanisms of sensing membrane curvature and stress-induced membrane curvature is important for the recruitment of autophagy machinery to form autophagosomes[61,62], a plausible hypothesis is that membrane depolarization and the subsequent membrane curvature may allow the integration of the myristic acyl-chain into damage sites. Indeed, CCCP-induced mitochondrial fragmentation is characterized by the formation of circular mitochondria (Supplementary Fig. 1J), which markedly increases the surface areas of the mitochondrial membrane and alters the curvature of the membrane both of which may increase the integration of *N*-myristoylated AMPK complex into the mitochondrial membrane.

In addition to AMPK, the AMPK kinase LKB1 is also regulated by protein lipidation with prenylation of LKB1 targeting its C-terminal cysteine residue within the CaaX motif. LKB1 prenylation appears to be crucial for the ability of LKB1 to activate AMPK[63]. Intriguingly, our data suggest that the role of AMPK in selective removal of damaged mitochondria is independent of the canonical energy-sensing function that requires functional LKB1. Thus, the different types of lipidation appear to play a critical role in determining AMPK function potentially by compartmentalizing AMPK to distinct membrane structures, as the membrane affinity of lipids varies depending on their acyl-chain lengths[64].

Since surveillance of damaged mitochondria plays a role in sustaining cancer cell viability by pre-empting the intrinsic apoptosis pathway, the underlying mechanisms could represent intervention targets for cancer treatment. Before our study, drugs that inhibit protein *N*-myristoylation, which is increased in a variety of cancers, have been assessed in preclinical studies[65]. It is poorly understood, however, whether individual myristoylated proteins can be targeted specifically. Our data suggest that AMPK is specifically regulated by NMT1 but not NMT2 despite both enzymes being expressed in lung cancer cells. NMT1 mRNA is overexpressed in ~34% of lung adenocarcinomas and correlates with worsened patient outcome with a 1.5-year reduction in median patient survival. Further, inhibition of

protein *N*-myristoylation is effective in eliminating lung cancer cells at least in cell culture and sensitizes lung cancer cells to sub-lethal doses of etoposide, providing a proof of concept for targeting protein *N*-myristoylation for lung cancer treatment. Future drug-discovery studies are warranted to identify NMT1-specific inhibitors, which may expand the therapeutic arsenal for lung cancer and other cancers, where high NMT1 mRNA levels are also associated with poorer patient outcomes.

Methods

Cell culture and treatment. Normal, ATG5$^{-/-}$ and AMPK$\alpha^{-/-}$ (deleted of both α1 and α2 catalytic subunits) MEFs obtained from Noboru Mizushima (Tokyo Medical and Dental University) and Keith R. Laderoute (SRI International, CA, USA), respectively, were maintained in DMEM with high glucose supplemented with 5% fetal bovine serum. Human cancer lines of the breast (MCF7 and MDA-MB231), lung (H23 and H226) and ovary (SKOV3) were cultured in RPMI1640 medium supplemented with L-glutamine and 5% fetal bovine serum. Where indicated cells were treated with rapamycin (Cell Signaling, Beverly, MA, USA), CCCP (Sigma-Aldrich, St Louis, MO, USA), and MK2206 (Whitehouse Station, NJ, USA). Control cells were incubated with vehicle (dimethylsulphoxide) only. Cell proliferation/viability was determined by incubation with 3-(4,5-dimethylthiazol-2-yl)-2,5-diphenyltetrazolium bromide (MTT) for 2h, followed by lysis in acidic isopropanol (0.35% HCl in isopropanol) and measurement of absorbance at 570 nm[66].

Plasmids and transfections. GFP- and RFP-AMPKα2 were generated by inserting human AMPKα2 coding complementary DNA amplified from a construct obtained from Anne Brunet (Stanford, CA, USA), verified by full-length sequencing. mCherry-p62 and GFP-LC3B were gifts from Terje Johansen (Norwegian Radium Hospital, Oslo, Norway) and Noboru Mizushima (Tokyo Metropolitan Instutite of Medical Science, Tokyo, Japan), respectively. AMPKβ1-GFP and AMPKβ1G2A-GFP were obtained from Jonathan S. Oakhill (University of Melbourne, Australia). TOM20-GFP was obtained from Origene (Rockville, MD, USA) and was used to construct TOM20-mCherry. Mito-AMPKβ1-GFP was constructed by N terminally tagging the mitochondrial localization signal of TOM20 amplified by PCR. Transfection was performed using FuGene 6 (Roche Scientific) for cancer cells and Lipofectamine LTX with PLUS (Invitrogen, Carlsbad, CA, USA) for MEFs according to the manufacturer's instructions and stable lines are established by G418 selection.

Antibodies, immunoprecipitation and western blotting. Antibodies to PARP, caspase 3, AKT, phospho-AKT (S473), phospho-AKT (T308), ribosomal protein S6 (S6), phospho-S6 (S240/244), PDK1, ULK1, phopsho-ULK1 (S467), phospho-ULK1 (S555), p62/SQSTM1, ATG5, ATG12, ATG14/barkor, VPS34, phospho-ACC, AMPKα, phospho-AMPKα (T172), LC3B and AMPKβ1/2 were obtained from Cell Signaling Technology; to ERK2, TOM20 (F10), TOM20 (FL-145), AMPKα (D6) and LKB1 (Ley37D/G6) from Santa Cruz Biotechnology (Santa Cruz, CA, USA); to ubiquitin (05–944) from Millipore (Billerica, MA, USA); to TSC2 and PARK2 (Parkin) from Epitomics (Burlingame, CA, USA); to LC3B from Novus Biologicals (Littleton, CO, USA); to ATG16L from MBL International (Woburn, MA, USA); to PARK2 anf PINK1 from Abcam (Cambridge, MA, USA); and to FIP200, VPS15 and rubicon from Bethyl Laboratories (Montgomery, TX, USA). Anti-phospho-ULK1 (S777) was a gift from Biomyx (San Diego, CA, USA). Antibodies to mitochondrial proteins used in RPPA were from MitoSciences (Eugene, OR, USA). Cell lysis and immunoblotting were performed as described previously[67] using 50 μg of protein lysates and equal protein loading was verified by blotting ERK2 (tumor lines) or CDK4 (MEFs). Antibodies to actin and LC3B were used at 1:5,000; to TOM20 and ERK2 at 1:2,000; and to the rest proteins at 1:1,000 dilutions for western blot. AMPK immunoprecipitation was performed using 1 mg protein lysate and a mouse monoclonal AMPKα antibody (D6). Mitochondrial isolation was performed using a Mitochondrial Isolation Kit from MitoSciences according to manufacturer's protocol. GFP-TRAP assays were performed using Chromoteck-GFP-Trap coupled to agarose beads from Allele (San Diego, CA, USA) according to the manufcaturer's protocol. Uncropped scans for the most important blots were presented in Supplementary Fig. 7.

RNAi. ON-TARGETplus siRNAs targeting human AMPKα (PRKAA1, 06-CCA UAC CCU UGA UGA AUU, 07-GCC CAG AGG UAG AUA UAU G, 08-GAG GAU CCA UCA UAU AGU U, 09-ACA AUU GGA UUA UGA AUG G; PRKAA2, 06-CGA CUA AGC CCA AAU CUU U, 07-GAG CAU GUA CCU ACG UUA U, 08-GAC AGA AGA UUC GCA GUU U, 09-GUC UGG AGG UGA AUU AUU U), NMT1 (12-UGG AGA AAC GCA AAC GGA GA, 11-UAA UGG AGU UAA CGG GUG A, 10-CAG CCA AGU GAC CGG GCA A, 09-CUG CAG CGA UUG CGA GAA U) and NMT2 (09-CCA GGA CAC GUG CGG GAU A, 10-GCA CAU UAU UGA CAC GUU U, 11-UAU CAA AUC AGU UCG AGA A, 12-CAU AAG AAG UUG AGA UCG A) were from Dharmacon (Lafayette, CO, USA). RNAi silencing was performed according to the manufacturer's protocol as described previously[68]. Stable LKB1 knockdown was performed using pre-made lentiviral shRNA constructs targeting LKB1 (sh-LKB1) from Open Biosystems (Huntsville, AL, USA). A non-targeting construct in the same vector system (pLKO.1) was used for control. Lentivirus stocks were prepared following the manufacturer's protocol. Briefly, 1.5×10^6 293T cells were plated in 10-cm dishes. Cells were co-transfected with shRNA constructs (3 μg) together with 3 μg pCMV-dR8.2 dvpr and 0.3 μg pCMV-VSV-G helper constructs from Addgene (Cambridge, MA, USA). Two days later, viral stocks were harvested from the culture medium, filtered and used to infect SKOV3 cells in the presence of 10 μg ml^{-1} polybrene. Stably infected cells were obtained by selection with 0.375–1 μg ml^{-1} of puromycin for 4 weeks.

Immunofluorescence, co-focal and electron microscopy. Immunofluorescent staining, phase contrast, fluorescence microscopy were performed as described previously[5,69]. For transmission electron microscopy, samples were fixed with 0.1 mol l^{-1} cacodylate buffer (pH 7.3) containing 3% glutaraldehyde and 2% paraformaldehyde for 1 h, washed and treated with 0.1% Millipore-filtered cacodylate-buffered tannic acid, postfixed with 1% buffered osmium tetroxide for 30 min and stained *en bloc* with 1% Millipore-filtered uranyl acetate. The samples were then dehydrated in increasing concentrations of ethanol, infiltrated and embedded in Spurr's low-viscosity medium, followed by polymerization at 70 °C for 2 days. Ultrathin sections were stained with uranyl acetate and lead citrate. A JEM 1010 transmission electron microscope (JEOL, USA) was used at an accelerating voltage of 80 kV and digital images were captured using the AMT Imaging System (Advanced Microscopy Techniques).

Reverse-phase protein microarray analysis. Tissue lysate microarray was processed as previously described[70]. Briefly, serially diluted lysates were spotted onto FAST slides (Schleicher & Schuell BioSciences, Keene, NH, USA) using a robotic GeneTAC arrayer (Genomic Solutions, Inc., Ann Arbor, MI, USA). After printing, the slides were blotted sequentially with Re-Blot (Chemicon, Billerica, MA, USA), I-Block and a biotin blocking system (Dako, Capinteria, CA, USA), probed with primary antibodies and incubated with biotin-conjugated secondary antibodies. The signals were then amplified using a Catalyzed Signal Amplification kit (DakoCytomation, Carpinteria, CA, USA) according to the manufacturer's instructions. The processed slides were scanned and quantified using the Microvigene software (VigeneTech Inc., North Billerica, MA, USA) and the quantitative values of 5 consistently expressed proteins (p38, JNK, ERK, mTor and GSK) as internal controls.

Bioorthogonal labelling and click chemistry. Cells were maintained in serum-free medium for 24 h before metabolic labelling with azidomyristate in the presence of 1% BSA (fatty acid free) using the Click-iT Metabolic Labelling kit (Life Technologies, Grand Island, NY, USA) according to the manufacturer's protocol. Following biotin conjugation, labelled proteins were detected by western blotting with streptavdin-HRP (Cell Signaling, Beverly, MA, USA).

References

1. Levine, B. & Klionsky, D. J. Development by self-digestion: molecular mechanisms and biological functions of autophagy. *Dev. Cell* **6,** 463–477 (2004).
2. Kroemer, G., Marino, G. & Levine, B. Autophagy and the integrated stress response. *Mol. Cell* **40,** 280–293 (2010).
3. Mizushima, N. & Levine, B. Autophagy in mammalian development and differentiation. *Nat. Cell Biol.* **12,** 823–830 (2010).
4. Lipinski, M. M. *et al.* A genome-wide siRNA screen reveals multiple mTORC1 independent signaling pathways regulating autophagy under normal nutritional conditions. *Dev. Cell* **18,** 1041–1052 (2010).
5. Liang, J. *et al.* The energy sensing LKB1-AMPK pathway regulates p27(kip1) phosphorylation mediating the decision to enter autophagy or apoptosis. *Nat. Cell Biol.* **9,** 218–224 (2007).
6. Hardie, D. G., Ross, F. A. & Hawley, S. A. AMPK: a nutrient and energy sensor that maintains energy homeostasis. *Nat. Rev. Mol. Cell Biol.* **13,** 251–262 (2012).
7. Mizushima, N. The role of the Atg1/ULK1 complex in autophagy regulation. *Curr. Opin. Cell Biol.* **22,** 132–139 (2010).
8. Wang, K. & Klionsky, D. J. Mitochondria removal by autophagy. *Autophagy* **7,** 297–300 (2011).
9. Kristensen, A. R. *et al.* Ordered organelle degradation during starvation-induced autophagy. *Mol. Cell Proteomics* **7,** 2419–2428 (2008).
10. Hailey, D. W. *et al.* Mitochondria supply membranes for autophagosome biogenesis during starvation. *Cell* **141,** 656–667 (2010).
11. Gomes, L. C., Di Benedetto, G. & Scorrano, L. During autophagy mitochondria elongate, are spared from degradation and sustain cell viability. *Nat. Cell Biol.* **13,** 589–598 (2011).
12. Rambold, A. S., Kostelecky, B., Elia, N. & Lippincott-Schwartz, J. Tubular network formation protects mitochondria from autophagosomal degradation during nutrient starvation. *Proc. Natl Acad. Sci. USA* **108,** 10190–10195 (2011).

13. Youle, R. J. & Narendra, D. P. Mechanisms of mitophagy. *Nat. Rev. Mol. Cell Biol.* **12,** 9–14 (2011).
14. Ashrafi, G. & Schwarz, T. L. The pathways of mitophagy for quality control and clearance of mitochondria. *Cell Death Differ.* **20,** 31–42 (2013).
15. Thomas, R. L. & Gustafsson, A. B. Mitochondrial autophagy. *Circ. J.* **77,** 2449–2454 (2013).
16. Semenza, G. L. Mitochondrial autophagy: life and breath of the cell. *Autophagy* **4,** 534–536 (2008).
17. Gegg, M. E. & Schapira, A. H. PINK1-parkin-dependent mitophagy involves ubiquitination of mitofusins 1 and 2: Implications for Parkinson disease pathogenesis. *Autophagy* **7,** 243–245 (2011).
18. Sarraf, S. A. *et al.* Landscape of the PARKIN-dependent ubiquitylome in response to mitochondrial depolarization. *Nature* **496,** 372–376 (2013).
19. Pankiv, S. *et al.* p62/SQSTM1 binds directly to Atg8/LC3 to facilitate degradation of ubiquitinated protein aggregates by autophagy. *J. Biol. Chem.* **282,** 24131–24145 (2007).
20. Matsuda, N. *et al.* PINK1 stabilized by mitochondrial depolarization recruits Parkin to damaged mitochondria and activates latent Parkin for mitophagy. *J. Cell Biol.* **189,** 211–221 (2010).
21. Ding, W. X. *et al.* Nix is critical to two distinct phases of mitophagy, reactive oxygen species-mediated autophagy induction and Parkin-ubiquitin-p62-mediated mitochondrial priming. *J. Biol. Chem.* **285,** 27879–27890 (2010).
22. Narendra, D., Kane, L. A., Hauser, D. N., Fearnley, I. M. & Youle, R. J. p62/SQSTM1 is required for Parkin-induced mitochondrial clustering but not mitophagy; VDAC1 is dispensable for both. *Autophagy* **6,** 1090–1106 (2010).
23. Rakovic, A. *et al.* Phosphatase and tensin homolog (PTEN)-induced putative kinase 1 (PINK1)-dependent ubiquitination of endogenous Parkin attenuates mitophagy: study in human primary fibroblasts and induced pluripotent stem cell-derived neurons. *J. Biol. Chem.* **288,** 2223–2237 (2013).
24. Van Laar, V. S. *et al.* Bioenergetics of neurons inhibit the translocation response of Parkin following rapid mitochondrial depolarization. *Hum. Mol. Genet.* **20,** 927–940 (2011).
25. Perez, F. A. & Palmiter, R. D. Parkin-deficient mice are not a robust model of parkinsonism. *Proc. Natl Acad. Sci. USA* **102,** 2174–2179 (2005).
26. Perez, F. A., Curtis, W. R. & Palmiter, R. D. Parkin-deficient mice are not more sensitive to 6-hydroxydopamine or methamphetamine neurotoxicity. *BMC Neurosci.* **6,** 71 (2005).
27. Sterky, F. H., Lee, S., Wibom, R., Olson, L. & Larsson, N. G. Impaired mitochondrial transport and Parkin-independent degeneration of respiratory chain-deficient dopamine neurons in vivo. *Proc. Natl Acad. Sci. USA* **108,** 12937–12942 (2011).
28. Aguiar, Jr. A. S. *et al.* Parkin-knockout mice did not display increased vulnerability to intranasal administration of 1-methyl-4-phenyl-1,2,3,6-tetrahydropyridine (MPTP). *Neurotox. Res.* **24,** 280–287 (2013).
29. Melrose, H. L., Lincoln, S. J., Tyndall, G. M. & Farrer, M. J. Parkinson's disease: a rethink of rodent models. *Exp. Brain. Res.* **173,** 196–204 (2006).
30. Grenier, K., McLelland, G. L. & Fon, E. A. Parkin- and PINK1-dependent mitophagy in neurons: will the real pathway please stand up? *Front. Neurol.* **4,** 100 (2013).
31. Dagda, R. K. *et al.* Mitochondrially localized PKA reverses mitochondrial pathology and dysfunction in a cellular model of Parkinson's disease. *Cell Death Differ.* **18,** 1914–1923 (2011).
32. Fu, M. *et al.* Regulation of mitophagy by the Gp78 E3 ubiquitin ligase. *Mol. Biol. Cell* **24,** 1153–1162 (2013).
33. Allen, G. F., Toth, R., James, J. & Ganley, I. G. Loss of iron triggers PINK1/Parkin-independent mitophagy. *EMBO Rep.* **14,** 1127–1135 (2013).
34. Ivatt, R. M. & Whitworth, A. J. The many faces of mitophagy. *EMBO Rep.* **15,** 5–6 (2014).
35. Strappazzon, F. *et al.* AMBRA1 is able to induce mitophagy via LC3 binding, regardless of PARKIN and p62/SQSTM1. *Cell Death Differ.* **22,** 419–432 (2014).
36. Hardie, D. G. AMP-activated/SNF1 protein kinases: conserved guardians of cellular energy. *Nat. Rev. Mol. Cell Biol.* **8,** 774–785 (2007).
37. Herrero-Martin, G. *et al.* TAK1 activates AMPK-dependent cytoprotective autophagy in TRAIL-treated epithelial cells. *EMBO J.* **28,** 677–685 (2009).
38. Kim, J., Kundu, M., Viollet, B. & Guan, K. L. AMPK and mTOR regulate autophagy through direct phosphorylation of Ulk1. *Nat. Cell Biol.* **13,** 132–141 (2011).
39. Egan, D. F. *et al.* Phosphorylation of ULK1 (hATG1) by AMP-activated protein kinase connects energy sensing to mitophagy. *Science* **331,** 456–461 (2011).
40. Hara, T. *et al.* Suppression of basal autophagy in neural cells causes neurodegenerative disease in mice. *Nature* **441,** 885–889 (2006).
41. Komatsu, M. *et al.* Loss of autophagy in the central nervous system causes neurodegeneration in mice. *Nature* **441,** 880–884 (2006).
42. Riley, B. E. *et al.* Ubiquitin accumulation in autophagy-deficient mice is dependent on the Nrf2-mediated stress response pathway: a potential role for protein aggregation in autophagic substrate selection. *J. Cell Biol.* **191,** 537–552 (2010).
43. Liang, J. & Mills, G. B. AMPK: a contextual oncogene or tumor suppressor? *Cancer Res.* **73,** 2929–2935 (2013).
44. Radoshevich, L. *et al.* ATG12 conjugation to ATG3 regulates mitochondrial homeostasis and cell death. *Cell* **142,** 590–600 (2010).
45. Pelicano, H. *et al.* Mitochondrial respiration defects in cancer cells cause activation of Akt survival pathway through a redox-mediated mechanism. *J. Cell Biol.* **175,** 913–923 (2006).
46. Behrends, C., Sowa, M. E., Gygi, S. P. & Harper, J. W. Network organization of the human autophagy system. *Nature* **466,** 68–76 (2010).
47. Shang, L. *et al.* Nutrient starvation elicits an acute autophagic response mediated by Ulk1 dephosphorylation and its subsequent dissociation from AMPK. *Proc. Natl Acad. Sci. USA* **108,** 4788–4793 (2011).
48. Moreno, D., Towler, M. C., Hardie, D. G., Knecht, E. & Sanz, P. The laforin-malin complex, involved in Lafora disease, promotes the incorporation of K63-linked ubiquitin chains into AMP-activated protein kinase beta subunits. *Mol. Biol. Cell* **21,** 2578–2588 (2010).
49. Oakhill, J. S. *et al.* beta-Subunit myristoylation is the gatekeeper for initiating metabolic stress sensing by AMP-activated protein kinase (AMPK). *Proc. Natl Acad. Sci. USA* **107,** 19237–19241 (2010).
50. Bijur, G. N. & Jope, R. S. Rapid accumulation of Akt in mitochondria following phosphatidylinositol 3-kinase activation. *J. Neurochem.* **87,** 1427–1435 (2003).
51. Miyamoto, S., Murphy, A. N. & Brown, J. H. Akt mediates mitochondrial protection in cardiomyocytes through phosphorylation of mitochondrial hexokinase-II. *Cell Death Differ.* **15,** 521–529 (2008).
52. Wang, X. *et al.* PINK1 and Parkin target Miro for phosphorylation and degradation to arrest mitochondrial motility. *Cell* **147,** 893–906 (2011).
53. Barretina, J. *et al.* The Cancer Cell Line Encyclopedia enables predictive modelling of anticancer drug sensitivity. *Nature* **483,** 603–607 (2012).
54. Mizushima, N. & Klionsky, D. J. Protein turnover via autophagy: implications for metabolism. *Annu. Rev. Nutr.* **27,** 19–40 (2007).
55. Reznick, R. M. & Shulman, G. I. The role of AMP-activated protein kinase in mitochondrial biogenesis. *J. Physiol.* **574,** 33–39 (2006).
56. Steinberg, G. R. & Kemp, B. E. AMPK in health and disease. *Physiol. Rev.* **89,** 1025–1078 (2009).
57. Canto, C. *et al.* AMPK regulates energy expenditure by modulating NAD + metabolism and SIRT1 activity. *Nature* **458,** 1056–1060 (2009).
58. Kim, J. *et al.* Differential regulation of distinct Vps34 complexes by AMPK in nutrient stress and autophagy. *Cell* **152,** 290–303 (2013).
59. Hanada, T. *et al.* The Atg12-Atg5 conjugate has a novel E3-like activity for protein lipidation in autophagy. *J. Biol. Chem.* **282,** 37298–37302 (2007).
60. Hedbacker, K., Townley, R. & Carlson, M. Cyclic AMP-dependent protein kinase regulates the subcellular localization of Snf1-Sip1 protein kinase. *Mol. Cell Biol.* **24,** 1836–1843 (2004).
61. Fan, W., Nassiri, A. & Zhong, Q. Autophagosome targeting and membrane curvature sensing by Barkor/Atg14(L). *Proc. Natl Acad. Sci. USA* **108,** 7769–7774 (2011).
62. Martin, D. D. *et al.* Identification of a post-translationally myristoylated autophagy-inducing domain released by caspase cleavage of Huntingtin. *Hum. Mol. Genet.* (2014).
63. Houde, V. P. *et al.* Investigation of LKB1 Ser431 phosphorylation and Cys433 farnesylation using mouse knockin analysis reveals an unexpected role of prenylation in regulating AMPK activity. *Biochem. J.* **458,** 41–56 (2014).
64. Hatzakis, N. S. *et al.* How curved membranes recruit amphipathic helices and protein anchoring motifs. *Nat. Chem. Biol.* **5,** 835–841 (2009).
65. Das, U., Kumar, S., Dimmock, J. R. & Sharma, R. K. Inhibition of protein N-myristoylation: a therapeutic protocol in developing anticancer agents. *Curr. Cancer Drug Targets* **12,** 667–692 (2012).
66. Vistica, D. T. *et al.* Tetrazolium-based assays for cellular viability: a critical examination of selected parameters affecting formazan production. *Cancer. Res.* **51,** 2515–2520 (1991).
67. Lu, Y. *et al.* Src family protein-tyrosine kinases alter the function of PTEN to regulate phosphatidylinositol 3-kinase/AKT cascades. *J. Biol. Chem.* **278,** 40057–40066 (2003).
68. Ding, Z. *et al.* Physical association of PDK1 with AKT1 is sufficient for pathway activation independent of membrane localization and phosphatidylinositol 3 kinase. *PloS One* **5,** e9910 (2010).
69. Xu, Z. X. *et al.* A plant triterpenoid, avicin D, induces autophagy by activation of AMP-activated protein kinase. *Cell Death Differ.* **14,** 1948–1957 (2007).
70. Sheehan, K. *et al.* Use of reverse phase protein microarrays and reference standard development for molecular network analysis of metastatic ovarian carcinoma. *Mol. Cell Proteomics* **4,** 346–355 (2005).

Acknowledgements

We are grateful to Noboru Mizushima for providing ATG5 knockout cells, to Keith R. Laderoute for providing AMPK knockout cells, to Jonathan S. Oakhill and Bruce E. Kemp for AMPKβ1 constructs, to Kenneth Dunner Jr. for expert support with electron

microscopy, to Wenbin Liu for analysing lung cancer data, and to Jordan U. Gutterman, Francois X. Claret and James R. Woodgett for helpful discussions. G.B.M. has received grant supports from National Cancer Institute (5 P30 CA016672 39 and 5 P50CA083639-15), Breast Cancer Research Foundation (01-06-00332) and Adelson Medical Research Foundation (00000196 and 00002690). Z.-X.X. has received grant supports from National Cancer Institute (R01CA133053) and a Career Development Award from the STI CRC NIH U19 AI 113212.

Author contributions

J.L. and G.B.M. conceived and designed the study and wrote the manuscript with contributions from all co-authors. J.L., Y.L. and Z.-X.X. performed the experiments with contributions from Q.Y., K.D.W., G.Z., G.P. and Z.D.; J.L., G.Z. and Y.L. performed statistical analysis with contributions from Y.-Y.P. and Z.D.; Y.L. and Q.Y. performed RPPA assays; Z.-X.X. and K.D.W. performed immunoflurence and cell viability assays; Z.-X.X. and G.Z. performed co-focal microscopy; Z.-X.X., Y.-Y.P., Z.D., M.J.G. and G.P. provided intellectual inputs.

Additional information

Supplementary Information accompanies this paper at http://www.nature.com/naturecommunications

Competing financial interests: The authors declare no competing financial interests.

Reprints and permission information is available online at http://npg.nature.com/reprintsandpermissions/

How to cite this article: Liang, J. *et al.* Myristoylation confers noncanonical AMPK functions in autophagy selectivity and mitochondrial surveillance. *Nat. Commun.* 6:7926 doi: 10.1038/ncomms8926 (2015).